Short Papers

The Finite-Element Method for Finding Modes of Dielectric-Loaded Cavities

J. P. WEBB, MEMBER, IEEE

Abstract—**A three-dimensional high-order finite-element scheme is proposed for finding the modes of dielectric-loaded cavities of arbitrary shape. New light is shed on the presence of spurious solutions. Results for an empty rectangular box are compared with exact solutions. A loaded rectangular box is also analyzed.**

I. Introduction

The analysis of dielectric-loaded cavities is important in the design of microwave filters [1] and ovens [2]. For all but the simplest three-dimensional configurations, this analysis must be done numerically. The lowest mode of a dilectric-loaded cavity has been determined by methods based on regular grid discretizations of Maxwell's equations [3],[4] and by a finite-element program designed for the solution of deterministic, rather than eigenvalue, problems [5]. More recently, Hara *et al.* [6] have used finite elements with an eigenvalue approach to find the modes of empty accelerator cavities.

The finite-element analysis of high-frequency electromagnetic problems is well known to be plagued by the occurrence of nonphysical, or spurious, solutions [7]–[10]. Such modes occur in abundance in the three-dimensional case, and, in [6], a modified functional is used to improve the situation by reducing the number of the spurious modes in the range of interest.

In this paper, the method of [6] is extended to allow for the solution of dielectric-loaded cavities. The variational formulation is given in Section II, where a more careful consideration of the modified functional provides a deeper understanding of the spurious modes produced. Section III gives a brief outline of the high-order tetrahedral elements. Results for the empty rectangular box are presented in Section IV, and for the dielectric-loaded box in Section V. A few remarks on the computational details are given in Section VI.

II. Variational Formulation

Let $\boldsymbol{H}(\boldsymbol{r})$ be the complex phasor magnetic field inside a cavity Ω, containing lossless materials with relative permittivity $\epsilon(r)$ and relative permeability $\mu=1$. Both materials properties are scalar functions of position only. Time dependence $e^{j\omega t}$ is assumed. Although in general $\boldsymbol{H}$ is complex, the resonant fields of a lossless, closed cavity are purely real, and henceforth $\boldsymbol{H}$ will be assumed to be real.

Let the boundary of Ω, $\partial\Omega$, be divided into two parts, $\partial\Omega_D$ and $\partial\Omega_N$. On $\partial\Omega_D$, the magnetic field satisfies the perfect magnetic conductor (Dirichlet) condition

$$\boldsymbol{H}\wedge\boldsymbol{n}=\boldsymbol{0} \tag{1}$$

where $\boldsymbol{n}$ is the unit outward normal to the surface $\partial\Omega$. On $\partial\Omega_N$, the magnetic field is free to vary.

Then the resonant modes of the cavity are the stationary points $\hat{\boldsymbol{H}}$ of the functional

$$F(\boldsymbol{H})=\int_\Omega\left\{\frac{1}{\epsilon}(\nabla\wedge\boldsymbol{H})^2-k^2\boldsymbol{H}^2\right\}dV. \tag{2}$$

(See, for example, [11].) The corresponding values of k are the normalized resonant frequencies of the cavity

$$k=\frac{\omega}{c} \tag{3}$$

where c is the velocity of light in free space. Furthermore, each modal field satisfies the perfect electric conductor (Neumann) boundary condition

$$(\nabla\wedge\boldsymbol{H})\wedge\boldsymbol{n}=\boldsymbol{0}\qquad\text{on }\partial\Omega_N. \tag{4}$$

This variational result has been used as the basic of a finite-element method for the determination of the modes of an empty cavity [6]. However, the method produces spurious modes along with the physical results, making the identification of the latter difficult. For this reason, the addition of a penalty term has been suggested [6] to enforce the solenoidality of the magnetic flux density (or, what amounts to the same thing in this case, the magnetic field). The modified functional is

$$F_m(\boldsymbol{H})=F(\boldsymbol{H})+s\int_\Omega(\nabla\cdot\boldsymbol{H})^2dV \tag{5}$$

where s is a positive real number. The use of this functional is found to reduce the number of spurious modes in the range of interest; furthermore, as s is increased, the spurious frequencies increase in value and can be forced up out of the range of interest.

More light may be shed on these facts by considering the Euler–Lagrange equation of (5). Let us first impose the boundary condition

$$\boldsymbol{H}\cdot\boldsymbol{n}=0\qquad\text{on }\partial\Omega_N. \tag{6}$$

Then it may readily be shown that the stationary points $\hat{\boldsymbol{H}}$ of (5) subject to (1) and (6) are the solutions to the equations

$$\nabla\wedge\frac{1}{\epsilon}\nabla\wedge\hat{\boldsymbol{H}}-s\nabla\nabla\cdot\hat{\boldsymbol{H}}-k^2\hat{\boldsymbol{H}}=0\qquad\text{in }\Omega \tag{7a}$$

$$\hat{\boldsymbol{H}}\wedge\boldsymbol{n}=\boldsymbol{0}\qquad\text{on }\partial\Omega_D \tag{7b}$$

$$\nabla\cdot\hat{\boldsymbol{H}}=0\qquad\text{on }\partial\Omega_D \tag{7c}$$

$$\hat{\boldsymbol{H}}\cdot\boldsymbol{n}=0\qquad\text{on }\partial\Omega_N \tag{7d}$$

$$(\nabla\wedge\hat{\boldsymbol{H}})\wedge\boldsymbol{n}=\boldsymbol{0}\qquad\text{on }\partial\Omega_N. \tag{7e}$$

To understand the solutions of (7), we define two additional sets of equations

$$\nabla\wedge\frac{1}{\epsilon}\nabla\wedge\hat{\boldsymbol{H}}-k^2\hat{\boldsymbol{H}}=0\qquad\text{in }\Omega \tag{8a}$$

$$\hat{\boldsymbol{H}}\wedge\boldsymbol{n}=\boldsymbol{0}\qquad\text{on }\partial\Omega_D \tag{8b}$$

$$(\nabla\wedge\hat{\boldsymbol{H}})\wedge\boldsymbol{n}=\boldsymbol{0}\qquad\text{on }\partial\Omega_N \tag{8c}$$

$$k^2>0 \tag{8d}$$

Manuscript received July 30, 1984; revised February 5, 1985. This work was supported in part by the Canadian Natural Sciences and Engineering Research Council.

The author is with the Department of Electrical Engineering McGill University, 3480 University St., Montreal, Quebec, Canada.

0018-9480/85/0700-0635$01.00 ©1985 IEEE

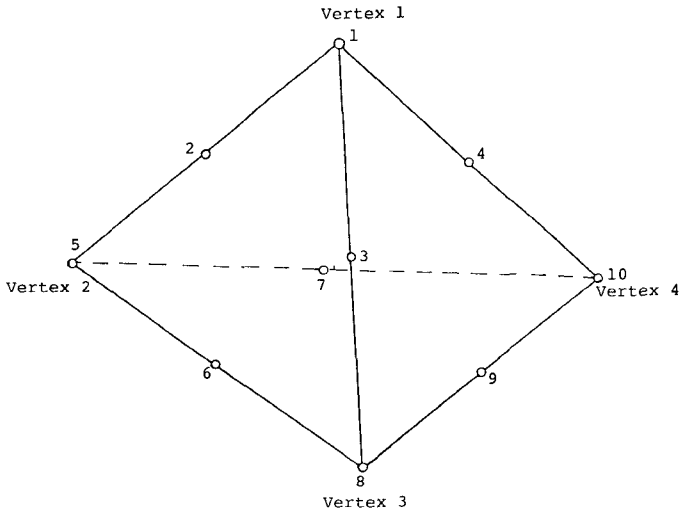

Fig. 1. A second-order tetrahedron, showing the ten interpolation nodes.

and

$$s\nabla\nabla\cdot\hat{\boldsymbol{H}} + k^2\hat{\boldsymbol{H}} = \boldsymbol{0} \quad \text{in } \Omega \tag{9a}$$

$$\hat{\boldsymbol{H}}\cdot\boldsymbol{n} = 0 \quad \text{on } \partial\Omega_N \tag{9b}$$

$$\nabla\cdot\hat{\boldsymbol{H}} = 0 \quad \text{on } \partial\Omega_D \tag{9c}$$

$$k^2 > 0. \tag{9d}$$

The solutions of (8) are the correct physical modes of the dielectric-loaded cavity with a perfect magnetic conductor along $\partial\Omega_D$ and a perfect electric conductor along $\partial\Omega_N$; (8a) is the curl–curl equation deducible directly from the time-harmonic Maxwell's equations.

The solutions of (9) have no obvious physical significance.

It is shown in the Appendix that each physical solution $(\hat{\boldsymbol{H}}, k^2)$ (that is, each solution to (8)) is also a solution to (7), and hence a stationary point of the modified functional (5). Similarly, each solution to (9) is a stationary point of the modified functional. So the modified functional possesses two sets of stationary points: a) one set are strictly solenoidal and are the physical modes of the cavity; b) the second set, governed by (9), are strictly irrotational nonphysical modes whose resonant frequencies increase linearly with the square root of the parameter s. These are the spurious modes previously noted [6],[7]. As s approaches zero, there will be infinitely many of these modes with vanishingly small frequency—this is what causes the trouble with the unmodified ($s = 0$) functional.

(It remains to be proven that the modified functional possesses no other solutions; the numerical results of the following sections suggest that it does not.)

Note that all of the above holds equally if we want to compute the electric field in a cavity containing variable-permeability materials, with a relative permittivity of 1.0; the functional is the one given by (2) and (5), but with ϵ replacing μ and $\boldsymbol{E}$ replacing $\boldsymbol{H}$.

III. Finite-Element Solution

The stationary points $(\hat{\boldsymbol{H}}, k)$ of (5) may be found approximately by the finite-element method. The following is similar to the numerical procedure given in more detail in [5].

The region Ω is broken into tetrahedral finite elements (see Fig. 1). In each element, the field $\boldsymbol{H}$ is approximated by a set of polynomials complete to order n (orders 1 to 3 have been implemented). Thus, for an nth -order tetrahedron

$$\boldsymbol{H}(\boldsymbol{r}) = \sum_{m=1}^{n_0} \boldsymbol{H}_m \alpha_m(\zeta) \tag{10}$$

where

$$n_0 = (n+1)(n+2)(n+3)/6$$

$$\zeta = (\zeta_1, \zeta_2, \zeta_3, \zeta_4)$$

$$= \text{simplex coordinates of point } \boldsymbol{r}$$

$$\alpha_m(\zeta) = \text{appropriate interpolation polynomials.}$$

For details of the simplex coordinates and interpolation polynomials, see [12]. $\boldsymbol{H}_m$ is the field at the mth node of the element; the nodes are spread through the element in a regular way (see Fig. 1).

The field is expressed in this manner in each element and nodal values are matched up at element interfaces. Then boundary conditions of the kind (1) and (6) are imposed. Currently, these may only be imposed on planes perpendicular to a Cartesian coordinate axis of the problem, but future developments will allow for more general boundaries. Suppose there are, finally, a total of N free field components at all the nodes of the region Ω. These free field components can be represented by a column vector $\boldsymbol{H}_c$, and (5) becomes (after some algebra)

$$F_M = \boldsymbol{H}_c^T \boldsymbol{W}_1 \boldsymbol{H}_c + s\boldsymbol{H}_c^T \boldsymbol{W}_2 \boldsymbol{H}_c - k^2 H_c^T \boldsymbol{W}_3 \boldsymbol{H}_c \tag{11}$$

where $\boldsymbol{W}_1$, $\boldsymbol{W}_2$, and $\boldsymbol{W}_3$ are $N \times N$ symmetric matrices.

Now since F_m must be stationary with respect to $\boldsymbol{H}_c$

$$(\boldsymbol{W}_1 + s\boldsymbol{W}_2)\boldsymbol{H}_c = k^2 \boldsymbol{W}_3 \boldsymbol{H}_c \tag{12}$$

which is a generalized algebraic eigenvalue problem for $(\boldsymbol{H}_C, k^2)$.

IV. Test Case: Empty Box

As a simple example, consider the problem of finding the resonant modes of the empty rectangular cavity Ω shown in Fig. 2. The walls $\partial\Omega$ of the cavity are perfectly conducting, so the governing equations for the electric field are

$$\nabla\wedge\nabla\hat{\boldsymbol{E}} - k^2\hat{\boldsymbol{E}} = 0 \quad \text{in } \Omega \tag{13a}$$

$$\hat{\boldsymbol{E}}\wedge\boldsymbol{n} = 0 \quad \text{on } \partial\Omega = \partial\Omega_D. \tag{13b}$$

The analytical solution to this problem is well known [13]; it consists of two sets of modes labelled TE_{mnp} and TM_{mnp}. The first set of modes have no z-component of electric field; the second set, no z-component of magnetic field. m, n, and p are nonnegative integers. The corresponding resonant frequencies are

$$k^2 = \pi^2\left(\frac{m^2}{a^2} + \frac{n^2}{b^2} + \frac{p^2}{c^2}\right). \tag{14}$$

In solving (13) with the electric-field version of the functional (5), we compute also a set of spurious solutions, whose governing equations are (from (9))

$$s\nabla\nabla\cdot\hat{\boldsymbol{E}} + k^2\hat{\boldsymbol{E}} = 0 \quad \text{in } \Omega \tag{15a}$$

$$\nabla\cdot\hat{\boldsymbol{E}} = 0 \quad \text{on } \partial\Omega = \partial\Omega_D. \tag{15b}$$

The analytical solution to this problem may readily be found; it consists of a single set of modes labelled S^E_{mnp}, with corresponding resonant frequencies given by

$$k^2 = s\pi^2\left(\frac{m^2}{a^2} + \frac{n^2}{b^2} + \frac{p^2}{c^2}\right). \tag{16}$$

The modes S^E_{mnp} are only nonzero if m, n, and p are all positive.

The problem was solved using the finite-element method described above, with 135 second-order tetrahedra. Table I gives the first six modes computed from this model, together with the analytical solution from (14) and (16).

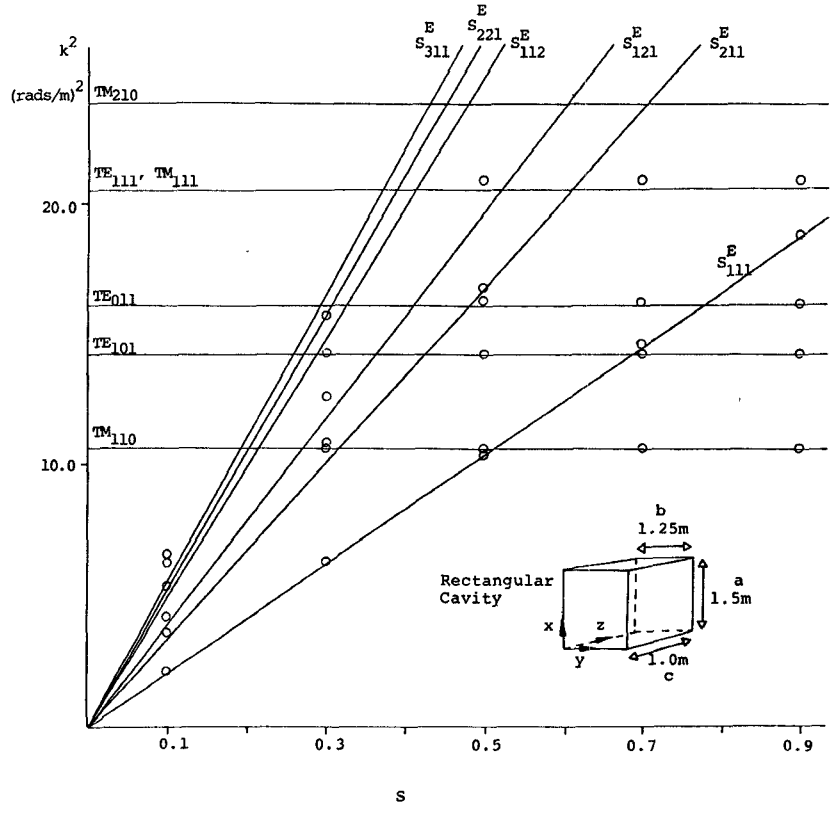

Fig. 2. The first six computed values of k^2 (○), plotted against the parameters s, for an empty rectangular box (inset); analytic results (———) were obtained from (14) and (16).

TABLE I.
RESONANT FREQUENCIES k (rads/m) FOR THE FIRST SIX MODES OF THE RECTANGULAR CAVITY SHOWN IN FIG. 2; $s = 0.4$

Finite Element Solution	Mode	Analytical Solution	Percent Error
2.8946	S^E_{111}	2.8686	0.9
3.2799	TM_{110}	3.2716	0.3
3.7843	TE_{101}	3.7757	0.2
3.7954	S^E_{211}	3.6733	3.3
4.0320	TE_{011}	4.0232	0.2
4.0973	S^E_{121}	3.9760	3.1

Fig. 2 shows the effect of varying s: the spurious values of k^2 vary linearly with s, while the true modes are unaffected by s.

V. DIELECTRIC-LOADED BOX

An irreducibly three-dimensional problem shown in Fig. 3 was solved using 135 second-order tetrahedra, at $s = 1.5$, for a variety of values of the ratio u/c. Two symmetry plans were used, one perpendicular to the x-axis and one perpendicular to the z-axis. The magnetic field was found.

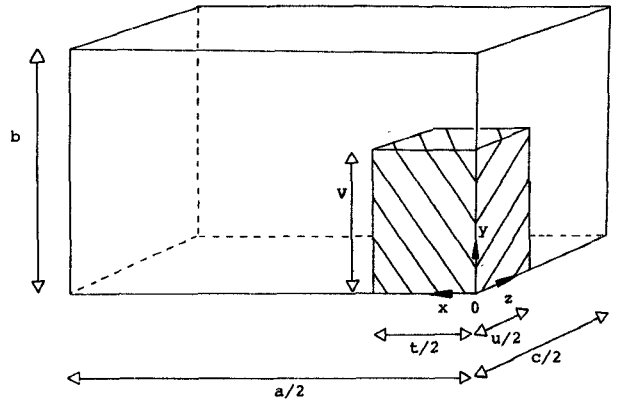

Fig. 3. One quarter of the problem of a dielectric block (relative permittivity 16) in rectangular box. $a = 1.0$ m, $b = 0.6$ m, $c = 0.2$ m, $t = 0.25$ m, $V = 0.35$ m, u varies from 0.0 m to 0.2 m. The walls $x = 0$ and $z = 0$ are planes of symmetry; the remaining walls of the box are perfect conductors.

In Fig. 4, the resonant frequencies of the first six modes are plotted against u/c. Table II compares the resonant frequency of the lowest mode, at $u/c = 0.375$, with values obtained by different methods. Note that, with the magnetic-field boundary conditions on the conducting cavity walls, the spurious modes are different to those of Section IV but just as straightforward to compute in closed form. They are labelled S^H_{mnp}, where now one of the indices m, n, or p may be zero.

VI. COMPUTATIONAL REMARKS

The algebraic eigenvalue problem (12) is large and sparse and only the first eigenpairs are required. An efficient method for this type of problem is that of trace minimization [14], and a solver

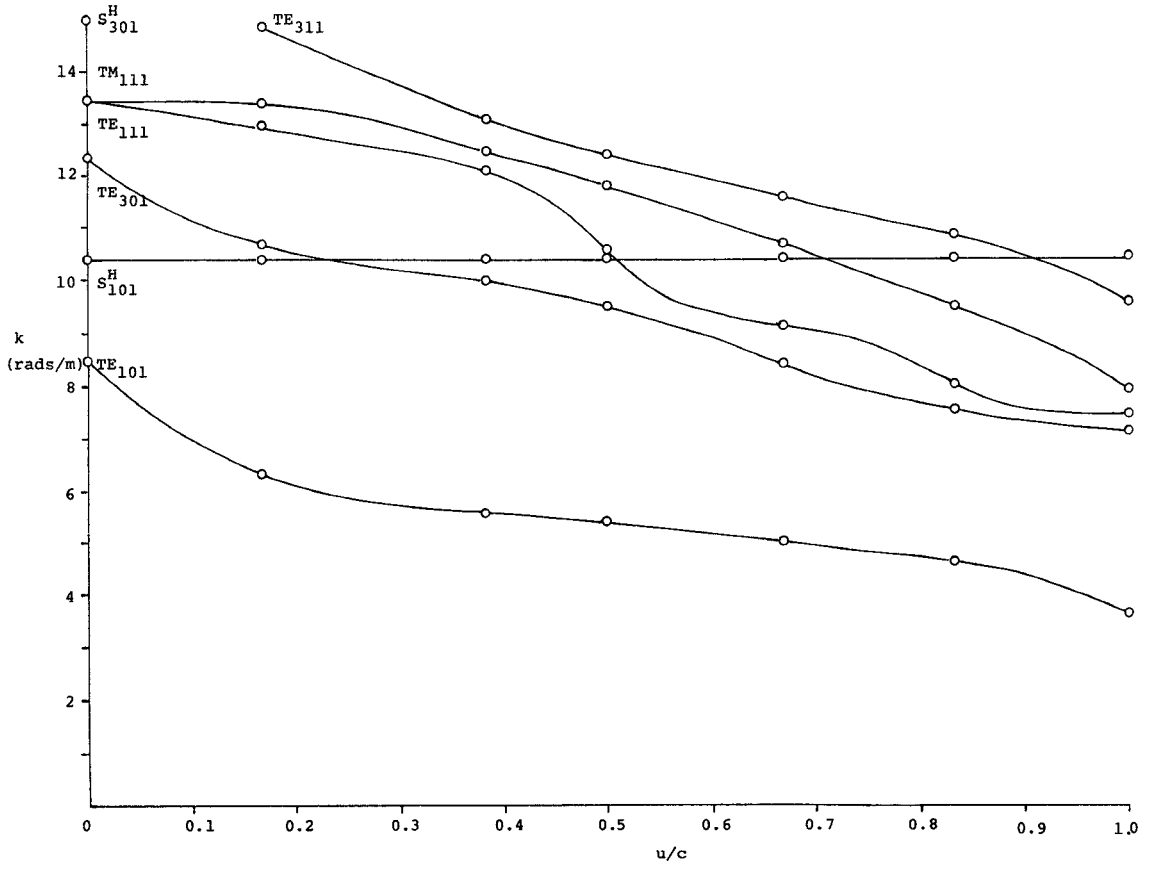

Fig. 4. The resonant frequencies k of the first six modes of a dielectric-loaded box (Fig. 3); $s = 1.5$.

TABLE II
RESONANT FREQUENCIES k (rads/m) OF THE LOWEST MODE OF THE DIELECTRIC-LOADED BOX SHOWN IN FIG. 3, WITH $u/c = 0.375$; $s = 1.5$

Source	Resonant Frequency	Estimated Percent Error
Ref. [3]	4.907	8.0
Ref. [4]	5.529	< 1.0
Ref. [5]	5.580	
This Method	5.621	< 1.0

based on this technique was built and used to obtain the above results. Typically, the matrices in (12) had dimensions of 400–500, but because the trace minimization algorithm requires only the nonzeros of the matrices to be stored in core, it was possible to obtain the solutions on minicomputers (PERQ and CODATA).

VII. CONCLUSIONS

High-order tetrahedral finite elements have been used to find the first few resonant modes of dielectric-loaded cavities. The modified functional [6] has been shown to possess a second set of nonphysical modes in addition to the physical solutions.

The modified functional approach, although enabling solutions to be computed, still has the undesirable feature that the optimum value of the parameter s for a particular problem is unknown, and must be guessed by the user before the computation begins, or determined by repeated solution (an expensive process).

APPENDIX
PROOF THAT A SOLUTION TO (8) IS ALSO A SOLUTION TO (7)

Let $\hat{\boldsymbol{H}}$, k^2 be a solution to (8). Then, from (8d), since $k^2 > 0$, (8a) gives

$$\nabla \cdot \hat{\boldsymbol{H}} = 0 \qquad \text{in } \Omega$$

and it follows that $\hat{\boldsymbol{H}}$, k^2 also satisfies (7a), (7b), (7c), and (7e). Furthermore

$$(\nabla \wedge \hat{\boldsymbol{H}}) \wedge \boldsymbol{n} = \boldsymbol{0} \qquad \text{on } \partial\Omega_N \Rightarrow$$

$$\left(\frac{1}{\epsilon} \nabla \wedge \hat{\boldsymbol{H}}\right) \wedge \boldsymbol{n} = \boldsymbol{0} \qquad \text{on } \partial\Omega_N \Rightarrow$$

$$\left(\nabla \wedge \frac{1}{\epsilon} \nabla \wedge \hat{\boldsymbol{H}}\right) \cdot \boldsymbol{n} = 0 \qquad \text{on } \partial\Omega_N \Rightarrow$$

$$\hat{\boldsymbol{H}} \cdot \boldsymbol{n} = 0 \qquad \text{on } \partial\Omega_N \quad \text{(from (8a))}$$

and so $\hat{\boldsymbol{H}}$ satisfies (7d) also.

REFERENCES

[1] S. J. Fiedzuisko, "Dual-mode dielectric resonator loaded cavity filters," *IEEE Trans. Microwave Theory Tech.*, vol. MTT-30, pp. 1311–1316, Sept. 1982.
[2] T. G. Mihran, "Microwave oven mode tuning by slab dielectric loads," *IEEE Trans. Microwave Theory Tech.*, vol. MTT-26, pp. 381–387, 1978.
[3] M. Albani and P. Bernardi, "A numerical method based on the discretization of Maxwell's equations in integral form," *IEEE Trans. Microwave Theory Tech.*, vol. MTT-22, pp. 446–450, Apr. 1974.
[4] S. Akhtarzad and P. B. Johns, "Solution of Maxwell's equations in three space dimensions and time by the t.l.m. method of numerical analysis," *Proc. Inst. Elec. Eng.*, vol. 122, pp. 1344–1348, Dec. 1975.

[5] J. P. Webb, G. L. Maile, and R. L. Ferrari, "Finite element solution of three-dimensional electromagnetic problems," *Proc. Inst. Elec. Eng.*, vol. 130, pt. H, no. 2, pp. 153–159, Mar. 1983.
[6] M. Hara, T. Wada, T. Fukasawa, and F. Kikuchi, "Three dimensional analysis of RF electromagnetic fields by finite element method," *IEEE Trans. Magn.*, vol. MAG-19, no. 6, pp. 2417–2420, 1983.
[7] J. B. Davies, F. A. Fernandez, and G. Y. Philippou, "Finite element analysis of all modes in cavities with circular symmetry," *IEEE Trans. Microwave Theory Tech.*, vol. MTT-30, pp. 1975–1980, Nov. 1982.
[8] B. M. A. Rahman and J. B. Davies, "Finite-element analysis of optical and microwave problems," *IEEE Trans. Microwave Theory Tech.*, vol. MTT-32, pp. 20–28, Jan. 1984.
[9] Z. J. Csendes and P. Silvester, "Numerical solution of dielectric loaded waveguides: I—Finite element analysis," *IEEE Trans. Microwave Theory Tech.*, vol. MTT-18, pp. 1124–1131, Dec. 1970.
[10] A. Konrad, "Vector variational formulation of electromagnetic fields in anisotropic media," *IEEE Trans. Microwave Theory Tech.*, vol. MTT-24, pp. 553–559, 1976.
[11] A. D. Berk, "Variational principles for electromagnetic resonators and waveguides," *IRE Trans. Antennas Propagat.*, vol. AP-4, pp. 104–110, Apr. 1956.
[12] P. Silvester and R. L. Ferrari, *Finite Elements for Electrical Engineers*. Cambridge, England: Cambridge University Press, 1983.
[13] S. Ramo, J. R. Whinnery, and T. Van Duzer, *Fields and Waves in Communication Electronics*. New York: Wiley, 1965.
[14] A. H. Sameh and J. A. Wisniewski, "A trace of minimization algorithm for the generalized eigenvalue problem," *SIAM J. Numer. Anal.*, vol. 19, no. 6, pp. 1243–1259, Dec. 1982.

Large-Signal Microwave Performance Prediction of Dual-Gate GaAs MESFET Using an Efficient and Accurate Model

ASHER MADJAR, SENIOR MEMBER, IEEE,
AND JONA DREIFUSS

Abstract—**This paper presents a microwave large-signal model for the dual-gate MESFET. The model enables prediction of device performance in small-signal and large-signal circuits. The model is an extension of a previously developed model for the ordinary MESFET. It relies on basic principles, thus correlating the device geometry and physical parameters to its performance. The speed and accuracy of the model are demonstrated by calculating three types of device performances: dc curves, small-signal scattering parameters, and large-signal simulation of an amplifier. Good agreement was achieved between calculated and measured performance. The computed results are presented for comparison only, and no attempt was made to present a comprehensive analysis of the device performance.**

I. Introduction

Increasingly, dual-gate GaAs MESFET devices are finding use in microwave circuits. In recent years, many researchers have investigated the device properties and applications. The most useful applications which have emerged thus far are: AGC amplifiers, mixers (including self-oscillating) [1]–[3], active phase shifters [2], [4], frequency multipliers [2], [5], power combiners/dividers [6], and up converters [7].

Small-signal circuits can be conveniently analyzed and designed by use of measured scattering parameters. However, in most of the above applications, the device operates in a large-signal mode. Large-signal circuits can be built, of course, experimentally, but this involves much "cut and try" effort. The best approach to nonlinear circuit development is to design the circuit theoretically (approximate design is usually acceptable), build it, and fine-tune it to the desired performance. This latter approach requires an efficient and reasonably accurate model for the device.

This paper presents such a model for the dual-gate MESFET. Its speed and accuracy are demonstrated by calculating the device performance and comparing it to the measured performance presented in the manufacturer's data sheet.

Manuscript received February 21, 1984; revised February 11, 1985.
The authors are with RAFAEL, Electronics Division, P.O. Box 2250, 31021 Haifa, Israel.

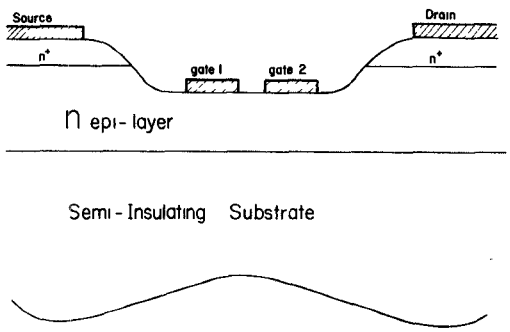

Fig. 1. Dual-gate MESFET cross-section view.

II. Device Structure

The physical structure of the device is presented in Fig. 1. As shown, the structure is similar to an ordinary FET except for the two gates. The device is built on a semi-insulating substrate of GaAs. An n-type epitaxial active layer is grown on the substrate, and on top of it an n^+ layer. The source and drain electrodes form ohmic contacts to the GaAs material, while the two gate electrodes form Schottky-barrier junctions.

From Fig. 1, it is obvious that this device is basically a combination of two ordinary MESFET's. In fact, Asai *et al.* [8], [9] have shown that electrically this device is a cascade connection of two ordinary FET's, the first in a common-source mode and the second in a common-gate mode. (See Fig. 3(a)).

III. The Model

An efficient and accurate microwave large-signal model for the ordinary MESFET was developed by Madjar and Rosenbaum [10]–[12]. This model was developed using basic principles, namely, solving the electric-field problem in the device in an approximate analytical fashion. This approach yielded a model which has advantages in all respects: it is fast, it related the physical device parameters to its electrical performance, and it has reasonable accuracy. The exact details of the model are presented in the above references.

The circuit diagram of an ordinary assembled FET is presented in Fig. 2. The "box" in the center of the diagram represents the active part of the device. This part is characterized by the computer model as follows:

$$I_g(t) = GVSG\frac{dV_{SG}(t)}{dt} + GVDS\frac{dV_{DS}(t)}{dt} \tag{1}$$

$$I_d(t) = I_{\text{con}} + DVSG\frac{dV_{SG}(t)}{dt} + DVDS\frac{dV_{DS}(t)}{dt}. \tag{2}$$

I_{con} and the four capacitive coefficients are functions of V_{SG}, V_{DS} and are computed by the model.

The other components in Fig. 2 are parasitic elements, which are undesirable but must be taken into account. The two diodes

0018-9480/85/0700-0639$01.00 ©1985 IEEE